JB
Journals.ASM.org

Genetic Dissection of T4 Lysis

Samir H. Moussa,[a,b]* Jessica L. Lawler,[c]* Ry Young[b,c]

Department of Biology, Texas A&M University, College Station, Texas, USA[a]; Center for Phage Technology, Texas A&M University, College Station, Texas, USA[b]; Department of Biochemistry and Biophysics, Texas A&M University, College Station, Texas, USA[c]

***t* is the holin gene for coliphage T4, encoding a 218-amino-acid (aa) protein essential for the inner membrane hole formation that initiates lysis and terminates the phage infection cycle. T is predicted to be an integral membrane protein that adopts an N^{in}-C^{out} topology with a single transmembrane domain (TMD). This holin topology is different from those of the well-studied holins S105 (3 TMDs; N^{out}-C^{in}) of the coliphage lambda and S68 (2 TMDs; N^{in}-C^{in}) of the lambdoid phage 21. Here, we used random mutagenesis to construct a library of lysis-defective alleles of *t* to discern residues and domains important for holin function and for the inhibition of lysis by the T4 antiholin, RI. The results show that mutations in all 3 topological domains (N-terminal cytoplasmic, TMD, and C-terminal periplasmic) can abrogate holin function. Additionally, several lysis-defective alleles in the C-terminal domain are no longer competent in binding RI. Taken together, these results shed light on the roles of the previously uncharacterized N-terminal and C-terminal domains in lysis and its real-time regulation.**

For most *Caudovirales*, a small phage-encoded membrane protein called the holin determines the timing of the onset of lysis and thus the length of the infection cycle (1). Holins are extremely diverse and populate at least three different topology classes (Fig. 1A). Most holins defined by experiment or by genomic analysis fall into classes I and II, with three and two transmembrane domains (TMDs), respectively (2–4). S105 and S68, the holins encoded by lambda and lambdoid phage 21, respectively, have been the experimental paradigms. Class III, populated with a single family of holins related to the holin T of phage T4, is unusual in that it has a large C-terminal periplasmic domain distal to its single TMD (5). Despite the topological and sequence diversity, holins share a set of characteristic functional features. From the onset of the viral morphogenesis period, the holins accumulate harmlessly in the cytoplasmic membrane until suddenly triggering at an allele-specific time (6). At the physiological level, triggering refers to the cessation of host respiration, depolarization of the membrane, escape of small cytoplasmic molecules to the medium, and loss of viability (6, 7). Triggering can also be induced by artificial depolarization of the membrane by energy poisons, leading to immediate premature lysis (7, 8).

Holins can be divided into two broad functional classes: canonical holins and pinholins (6). In cells where canonical holins have triggered, micrometer-scale lesions, or holes, are formed in the cytoplasmic membrane, typically 1 to 3 per cell (9, 10). In contrast, pinholin triggering results in the formation of ~10^3 heptameric "pinholes," estimated to have an ~2-nm lumen (11). Studies with green fluorescent protein (GFP) fusions of both holins and pinholins have revealed that the triggering event is associated with the sudden redistribution of the holin molecules from a mobile, uniformly distributed state, probably dominated by homodimers, into large, immobile two-dimensional aggregates (12). The general model is that triggering reflects the attainment of an allele-specific critical concentration in the membrane, after which nucleation of the large aggregates and hole formation rapidly ensue (1). The prevailing perspective, then, is that the length of the infection cycle is encoded in the primary structure of the holin (1). Phages can evolve to longer or shorter infection cycles by holin mutations; indeed, mutational studies of several different holins, including T, have shown that missense changes can lead to major alterations in the triggering time, either earlier or later in the infection cycle (2, 4, 5, 13).

The T4 *t* gene has a storied history. Early in the history of modern molecular genetics, a set of six genetic loci in the closely related T2 and T4 coliphages were identified by plaque morphology phenotypes and designated "*r*" for "rapid lysis" (14–16). We now know that the *r* phenotype reflects a defect in establishing or maintaining the state of lysis inhibition (LIN) (16). LIN is imposed when a T4-infected cell is superinfected by another T4 virion. Essentially, when this happens, the normal schedule for lysis is abrogated. The infection cycle is allowed to continue, resulting in the intracellular accumulation of more progeny virions (15). The molecular roles of two *r* loci, *rI* and *rV*, have been established (5). *rV* is allelic to *t*, whereas *rI* encodes the antiholin, RI. RI is secreted into the periplasm, where, if activated by the process of superinfection, it binds to the periplasmic domain of T and prevents triggering (5, 17).

As part of our long-term effort to understand how holins effect the tight temporal regulation of host lysis, we have focused on T as a regulatory paradigm. T exhibits all of the characteristic functional features of other canonical holins but is also subject to LIN, which is the only established example where environmental information is used to affect lysis timing (18). We have previously subjected *t* to genetic analysis by selecting for alleles with altered triggering times (5). Most of the altered-timing mutations mapped to the periplasmic domain. Despite the rich knowledge of the genetics of *t*, including our own efforts in identifying timing mutants, no collection of lysis-defective missense alleles exists (5). This has impeded both physiological and biochemical analysis of

Received 7 February 2014 Accepted 28 March 2014
Published ahead of print 4 April 2014
Address correspondence to Ry Young, ryland@tamu.edu.
* Present address: Samir H. Moussa, Department of Microbiology and Immunobiology, Harvard Medical School, Boston, Massachusetts, USA; Jessica L. Lawler, Program in Virology, Harvard Medical School, Boston, Massachusetts, USA.

doi:10.1128/JB.01548-14

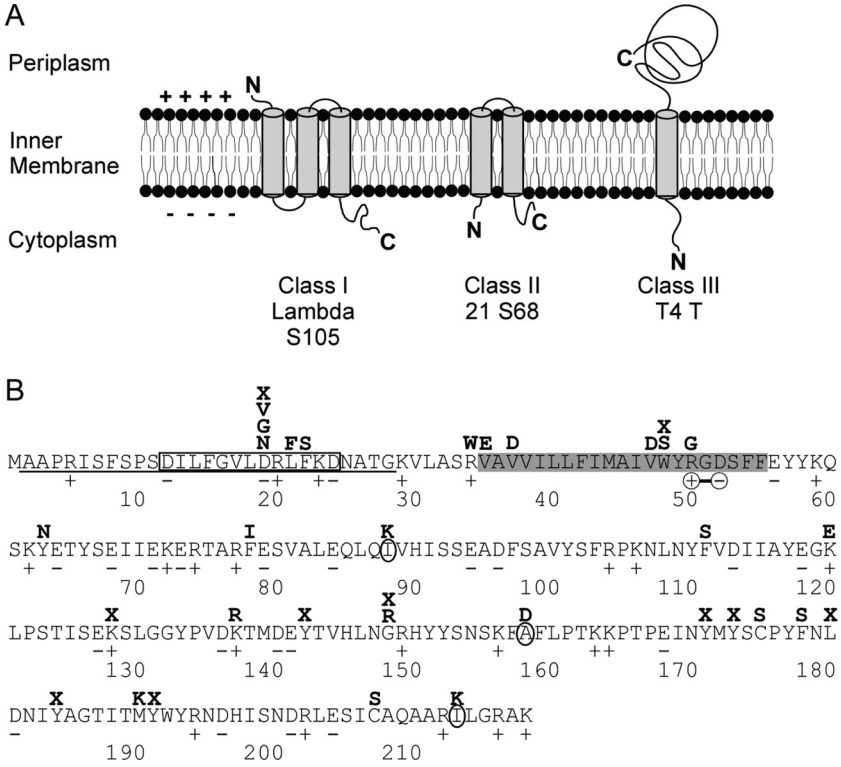

FIG 1 Lysis-defective missense mutations are obtained in all 3 topological domains of the T4 holin. (A) Prototypes of the experimentally confirmed holin topological classes. + and − indicate the polarity of the membrane potential. (B) Primary structure of the T4 holin, T, with lysis-defective missense and nonsense (X) alleles indicated. The N-terminal cytoplasmic domain is underlined, and the predicted amphipathic helix within the N-terminal domain is boxed. The predicted TMD is highlighted in gray, and the charges predicted to form a 1-3 salt bridge within the TMD are circled. Mutations that exhibit dominant negative character (I88K, A158D, and I213K) are circled in the C-terminal domain. Missense mutants D19N and D19G were collected in a previous study (5), while C175S and C207S were generated by site-directed mutagenesis in a previous study (20).

T. By comparison, many lysis-defective missense alleles have been identified for two other holins, lambda S105 and S68 (2, 4, 19). The analysis of these mutants, both *in vivo* and *in vitro*, has allowed the formulation of detailed molecular pathways for holin function (19). These considerations suggest that similar mechanistic insight for class III holins might derive from analysis of a collection of *t* lysis-defective alleles. Here we report efforts to generate and characterize such a collection. The results are discussed in terms of a model for T function and its regulation by RI.

MATERIALS AND METHODS

Bacterial strains, plasmids, bacteriophages, and culture growth. The bacterial strains, bacteriophages, and plasmids used in this study are described in Table 1. Bacterial cultures were grown in standard LB medium supplemented with ampicillin (100 μg ml^{-1}), kanamycin (40 μg ml^{-1}), and chloramphenicol (10 μg ml^{-1}) when appropriate. Growth and lysis of cultures were monitored by A_{550} as described previously (20). When indicated, isopropyl β-D-thiogalactopyranoside (IPTG), KCN, or $CHCl_3$ was added to give a final concentration of 1 mM, 10 mM, or 1%, respectively. For the dominance/recessiveness tests, CQ21 cells lysogenized with λ*t*, a derivative of lambda with the parental *t* holin gene substituted for *S* (18), were transformed with pSM-t* plasmids and induced at an A_{550} of 0.3 by a shift to 42°C. Experiments testing whether the mutant periplasmic domains were competent in binding RI were performed by infecting CQ21 cells carrying pZA-ssPhoAΦsT* with wild-type (WT) T4 at an A_{550} of ~0.2.

Error-prone PCR mutagenesis and selection for lysis-defective alleles of *t*. Error-prone PCR mutagenesis was performed using the GeneMorph II random mutagenesis kit, which was used with no modification from the manufacturer's instructions except for optimization of PCR cycle number and temperature conditions to maximize the number of alleles with single nucleotide changes. Oligonucleotides for PCR mutagenesis (Table 1) were obtained from Integrated DNA Technologies (Coralville, IA) and were used without further purification. Mutagenized PCR fragments of *t* were double digested using NcoI and BglII from New England BioLabs and ligated into the parental plasmid pSM-t with T4 ligase (NEB). This plasmid carries the lambda lysis cassette except that λ *S105* was replaced with T4 *t* and the *Rz/Rz1* spanin genes were deleted. Both *t* and *R*, encoding the lambda endolysin, are under the control of the pR′ promoter. *Escherichia coli* XL1 Blue cells were transformed with these mutagenized plasmids (pSM-t*), each transformant plate slurried (~500 colonies/plate), and plasmids purified using the Qiagen spin miniprep kit. *E. coli* MC4100 cells carrying a thermoinducible lambda lysogen [λcamΔ(*SR*)], defective in lysis, were transformed with the pSM-t* plasmid candidate *t* defective plasmids. In this system, the induction of the prophage provides the *Rz/Rz1* spanin function and transactivates the plasmid promoter, ensuring that the necessary lysis proteins (holin, endolysin, i-spanin, and o-spanin) are provided with physiologically relevant timing and expression levels. An initial enrichment for lysis-defective alleles was performed by slurrying a freshly transformed plate with ~500 transformant colonies with LB, dilution, and inoculation into 100 ml LB with appropriate antibiotics to a starting A_{550} of ~0.05. Cultures in LB broth supplemented with ampicillin were grown at 30°C to an A_{550} of 0.3, plasmids were induced by heat shift for 60 min, and nonlysed cells were collected by filtration. Plasmids of the collected cells were prepared using the Qiagen spin miniprep kit and used to transform MC4100 λcamΔ(*SR*) cells. Single colonies were picked, grown to an A_{550} of ~0.3 in 5 ml of LB supplemented with ampicillin at 30°C, induced by aerating at 42°C for 15

TABLE 1 Phages, strains, plasmids, and primers used in this study

Phage, strain, plasmid, or primer	Description or sequence	Source or reference
Phages		
T4, WT	Bacteriophage T4D	Lab stock
λΔ(*SR*)	Δ(*stf-tfa*)::*cat* cI857 Δ(*SR*)	Lab stock
Strains		
MC4100 Δ*tonA*	*E. coli* K-12 F *araD139* Δ(*argF-lac*)*U169 rpsL15 relA1 flbB3501 deo pstF25 rbsR tonA*	Lab stock
MC4100 λ*cam*Δ(*SR*)	MC4100 Δ*tonA* lysogenized with λΔ(*SR*)	Lab stock
CQ21 *recA srl*::Tn*10*	*E. coli* K-12 *ara leu lacI*^{q1} *purE gal his argG rpsL xul mtl ilv*	Lab stock
CQ21 λ*kan*Δ(SR) *recA srl*::Tn*10*	CQ21 lysogen carrying λ*kan*Δ(*SR*) prophage	Lab stock
SHuffle T7 [SHuffle(DE3)]	*E. coli K-12 fhuA2 lacZ*::*T7 gene1* [*lon*] *ompT ahpC gal* λ*att*::pNEB3–r1-cDsbC Δ*trxB sulA11 R*(*mcr-73*::miniTn*10*)*2* [*dcm*] *R*(*zgb-210*::Tn*10*) *endA1* Δ*gor* Δ(*mcrC-mrr*)*114*::IS*10*	New England Biolabs
Plasmids		
pER-t	Carrying lysis cassette of λ except *S* is replaced by T4 *t* gene	18
pER-t$^{\Delta 2\text{-}28}$	pER-t with residues 2–28 deleted in *t*	This study
pSM-t	pER-t with in-frame deletion of *Rz/Rz1* in the lysis cassette of λ	19
pSM-t*	pSM-t carrying lysis-defective mutations of *t*	This study
pZA-T	pZA32Δ*luc*::*t*	26
pZA-ssPhoAΦsT	Codons 1–55 in pZA-T replaced by codons 1–26 of *phoA*, encoding signal sequence	26
pZA-ssPhoAΦsT*	pZA-ssPhoAΦsT carrying lysis-defective mutations of *t* found in the periplasmic domain	This study
pET11a-sT^{his}	pET11a-T^{his} with deletion in codons 2–55 of *t*	19
pET11a-sT^{his} I88K	pET11a-T^{his} carrying I88K mutation	This study
Primers		
pSM-t mutate for	5′-CTTAAAAGGAGGGTCCATG-3′	
pSM-t mutate rev	5′-CTTTTTTAGCAGAGATCTAATAATTA-3′	

min, and then grown for 45 min more at 37°C. These cultures were assessed for lysis activity by monitoring culture growth throughout the induction period. $CHCl_3$ was added to each culture at the end of each experiment to ensure that the lack of lysis was due to a defective holin rather than to a defect in the expression of the *R* endolysin gene. Plasmids of defective *t* alleles were sequenced by Eton Biosciences (San Diego, CA) to determine the mutation responsible for the lysis-defective phenotype. While single, double, and triple missense and nonsense mutants were collected in this study, only single mutants were pursued.

TCA precipitation, subcellular fractionation, SDS-PAGE, and Western blotting. To quantify the amount of protein produced from pSM-t*, 10 ml of a culture induced for 15 min was collected, and 1.1 ml of 100% cold trichloroacetic acid (TCA) was added (10% final concentration), as described previously (20). Precipitates were collected by centrifugation at 7,000 rpm in a clinical centrifuge and washed in 5 ml of cold acetone, and pellets were dried. The pellets were resuspended in sample loading buffer containing 5% β-mercaptoethanol. Subcellular fractionation of cells, to determine whether the mutant *t* allele product was present in the membrane, was performed as previously described (21). Briefly, 25 ml of induced cultures was collected by centrifugation at 4,000 × *g* in a Sorvall Superspeed RC2-B centrifuge and resuspended in 2 ml of purification buffer (0.1 M sodium phosphate [pH 8.0], 0.1 M NaCl) supplemented with protease inhibitor cocktail (Sigma, St. Louis, MO) and 100 μg ml^{-1} final concentrations of DNase and RNase. Cells were disrupted in a French pressure cell at 16,000 lb/in^2, and the membrane and soluble fractions were separated by centrifugation at 100,000 × *g* in a Beckman TLA100.3 rotor for 60 min. Equivalent amounts of each fraction were examined by SDS-PAGE and Western blotting. SDS-PAGE and Western blotting were performed as previously described (20).

Blue-native PAGE. Blue-native PAGE was performed as previously described (19) with minor modifications. Cultures expressing wild-type *t* or its lysis-defective alleles were harvested at the wild-type lysis time (15 min after induction) and disrupted in a French pressure cell as described above. Membrane fractions were collected by ultracentrifugation in a 50.2 Ti rotor for 60 min at 100,000 × *g*. Membranes were resuspended with 1 ml extraction buffer (50 mM NaCl, 50 mM imidazole, 1 mM EDTA, 10% [vol/vol] glycerol, and 1% n-dodecyl-β-D-maltopyranoside) and extracted overnight at 4°C. Insoluble material was removed by ultracentrifugation at 100,000 × *g* in a TLA100.3 rotor for 60 min. A 20-μl aliquot of supernatant was mixed with 1 μl 5% (wt/vol) Coomassie brilliant blue G-250 (Bethesda Research Laboratories, MD) and loaded on a 4 to 16% native polyacrylamide gel (Invitrogen), with electrophoresis and Western blotting performed as described previously (19). The NativeMark (Invitrogen) molecular mass marker was used.

Gel filtration. Gel filtration chromatography was carried out using an analytical grade Superdex 75 or Superdex 200 column, calibrated with standards purchased from Bio-Rad, on an AKTA fast protein liquid chromatograph (FPLC). Columns were equilibrated with 20 column volumes of purification buffer with 1% *n*-dodecyl-β-D-maltopyranoside (DDM) before sample injection to show oligomerization of T in the membrane and purification alone to show oligomerization of the periplasmic domain of T (sT). Once sample was injected, gel filtration was performed at 0.4 ml min^{-1} until one column volume of buffer had eluted. Fractions were collected and analyzed by SDS-PAGE and Western blotting as described previously (20).

RESULTS

Missense mutations conferring defective lysis map to all 3 topological domains of the T holin. To obtain a pool of lysis-defective *t* mutants, the *t* gene was subjected to error-prone PCR mutagenesis. This pool of mutant DNAs was used to construct a library of medium-copy plasmids with the *t* gene cloned under the control of the λ late promoter, pR′. The library was first enriched for lysis-defective alleles (see Materials and Methods) and then screened for failure to complement a holin-defective lambda prophage (Fig. 2A). Using this screen, 59 lysis-defective alleles were identified (see Materials and Methods), among which 18 had two

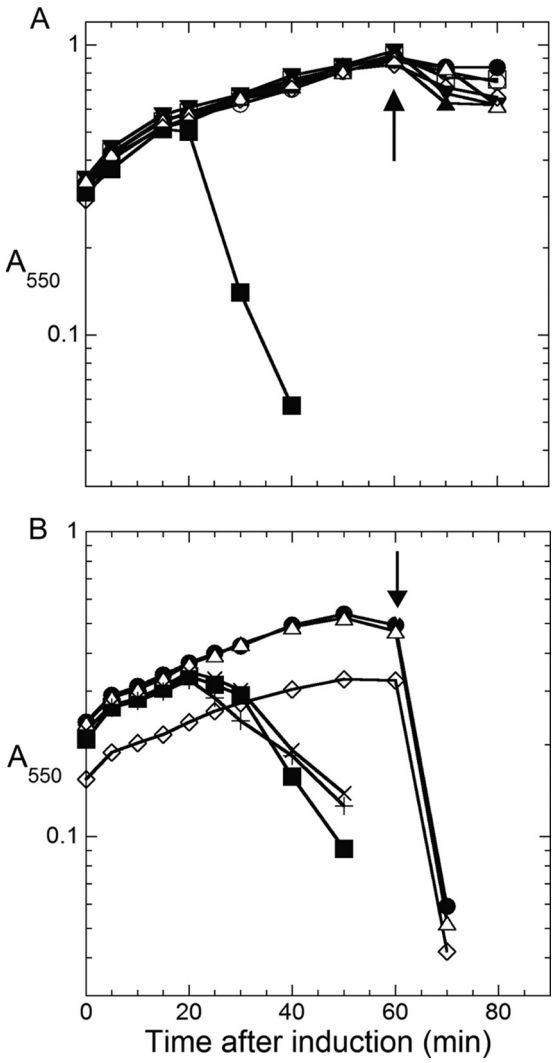

FIG 2 Lysis and LIN defect of *t* missense mutants. (A) Cells carrying the indicated *t* alleles in the context of the pSM-t plasmid were thermally induced in logarithmic growth at $t = 0$. ■, wild type; ●, D19am (negative control); ▲, L21F; ▼, F22S; □, V37D; ○, V47D; △, F111S; ◇, I213K. The arrow at 60 min indicates the addition of 10 mM (final concentration) KCN. (B) Lysis-defective alleles of *t* abrogate interactions with RI. Lysis indicates that the sT domain can bind RI, titrating it away from the full-length T encoded by the wild-type phage, while failure to undergo lysis indicates that the mutated periplasmic domain of T is not competent in RI binding. ■, wild type; ●, D19am (negative control); △, F111S; X, K120E; +, G148R; ◇, I213K. The arrow at 60 min indicates the addition of 1% (final concentration) $CHCl_3$.

or more missense changes and 20 had single missense alleles (Fig. 1B). The lysis-defective mutant hunt did not approach saturation for single missense changes, as judged by the fact that only 21 nonsense alleles (single [Fig. 1A] and as part of two or more missense changes [not shown]) were obtained out of 78 that could be expected from random single-base changes in the *t* reading frame. Nevertheless, missense mutations in all three topological domains of T were isolated and are considered below in each context.

The N-terminal cytoplasmic domain (residues 1 to 34) (T_{NTD}). Among the experimentally confirmed holins, all but T have a very short cytoplasmic domain, usually only a few residues at either N or C termini (1). Extensive mutational analysis of S105 and $S^{21}68$ has shown that these small cytoplasmic peptide sequences control the topology of the first TMD, and thus the lytic function of the holin, through the presence or absence of charged residues. In both cases, mutations that increase the positive charge in the short cytoplasmic domain change the membrane topology and cause a loss of lytic function (2, 4). T has a predicted 31-amino-acid (aa) cytoplasmic domain, easily the largest of any identified holin (1). Previously, the only two *t* missense changes conferring an absolute lysis defect, D19N and D19G, were also in the N-terminal cytoplasmic domain and also caused an increase in the net positive charge of the domain (5). However, selection using the PCR-mutagenized pool yielded three more lysis-defective mutants with mutations, D19V, L21F, and F22S, in the cytoplasmic domain. This brought the total to five independent lysis-defective mutants with missense changes clustered within a four residue stretch of the cytoplasmic domain. Secondary structure analysis using JPred (22) indicated that this sequence is predicted to form an amphipathic alpha helix (Fig. 3A); moreover, this predicted secondary structure is conserved in *t* genes from other phages. Taken together, these results suggest that the amphipathic helix is important for T hole formation. An allele in which the DNA encoding the cytoplasmic domain was deleted exhibited a drastic delay in the onset of lysis; moreover, even after triggering at ~80 min, lysis was much less rapid, despite having nearly an extra hour for accumulation of endolysin activity (Fig. 3B). To address whether this delayed lysis reflected nonspecific damage to the membrane consequent to overaccumulation of the T protein, KCN was added at a time ~20 min prior to the lysis time for the deletion allele. Addition of cyanide to depolarize the membrane causes instant triggering of all experimentally confirmed holins, but not lysis-defective variants (8), and thus can be used as an indicator of holin function. Here, the addition of KCN did result in a premature triggering response, as judged by the sudden decrease in turbidity, but the decrease in culture mass was even more gradual than that observed after the spontaneous triggering at 80 min. The simplest idea is that the holes formed by the TΔ2-28 protein are only partially permissive to the endolysin, indicating that the N-terminal cytoplasmic domain is important for both the timing and structure of the T holes. The third mutation in this domain is considered below.

The TMD (residues 35 to 55) (T_{TMD}). T is unambiguously an integral membrane protein (5). Nevertheless, most TMD prediction algorithms (23, 24) fail to identify a TMD in the T primary structure, because the longest stretch of hydrophobic sequence uninterrupted with charged residues is only 15 aa (Val36 to Trp49), which is considered too short for a TMD to span the bilayer. However, in an alpha helix, Arg50 and Asp52 could form a 1-3 salt bridge, as is seen at three positions in the TMDs of lambda S105 (2). Incorporating this salt bridge would allow the TMD to extend to a more reasonable length of 20 residues, extending through Phe55 (Fig. 1B). The mutations in this domain support the notion that the TMD spans this region (i.e., residues 35 through 55). V35E, V37D, and V47D would each directly introduce a charged residue and shorten or destroy the predicted TMD, whereas R50G would have the same effect indirectly, by eliminating the required salt bridge. W48S would also drastically reduce the hydrophobic character of the TMD. In contrast, the R34W mutation, rather than destroying the hydrophobic character of the TMD, would instead be predicted to reposition its cytoplasmic boundary a full turn of the TMD helix, possibly to Val30.

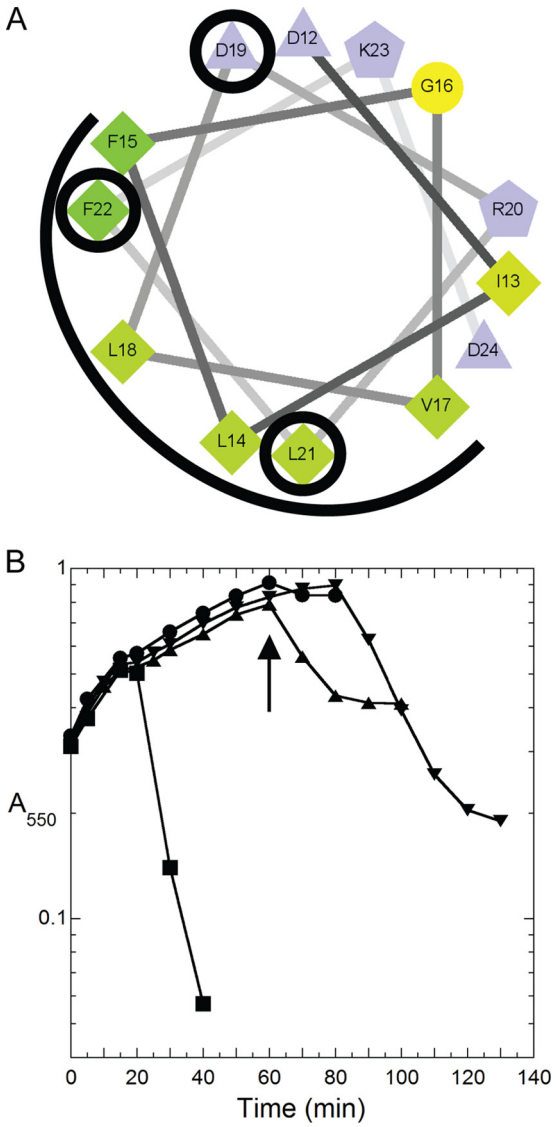

FIG 3 The N-terminal cytoplasmic domain of T contains a predicted amphipathic helix. (A) Helical-wheel projection of the predicted amphipathic helix from residues 12 to 24, with hydrophobic residues (diamonds), negatively charged residues (triangles), positively charged residues (pentagons), and weakly hydrophobic residues (circles) indicated. The hydrophobic face of the helix is indicated by an arc. Positions in the amphipathic helix that give rise to lysis-defective alleles are circled. (B) Deletion of the N-terminal cytoplasmic domain confers a partial lysis phenotype defective in both timing and lytic rate. ■, wild type; ●, D19am (negative control); ▼, $t_{\Delta 2\text{-}28}$; ▲, $t_{\Delta 2\text{-}28}$ with 10 mM (final concentration) KCN added at 60 min as indicated by the arrow.

This suggests that the positioning of the TMD with respect to the soluble cytoplasmic and periplasmic domains is critical.

The most striking aspect of this collection of mutants is the absence of lysis-defective mutants with conservative changes, i.e., changes that would not be predicted to alter the hydrophobic character or positioning of the TMD. In all other holin systems where lysis-defective missense alleles have been obtained, multiple alleles have been isolated with conservative changes within the TMD segments (4, 13). The simplest interpretation is that the TMD of the T holin is relatively less important in terms of the pathway to lethal hole formation.

The periplasmic domain (residues 56 to 216) (T_{CTD}). As the binding target of the T4 antiholin, RI, the soluble periplasmic domain of T has been subjected to extensive analysis independent of its context in the full-length protein (20, 25, 26). Heterodimeric complexes between the periplasmic domains of RI and T have been purified and characterized (20). In the absence of RI, T_{CTD} rapidly oligomerizes (20). Thirteen lysis-defective missense changes were found in this domain (Fig. 1B). However, unlike the lysis-defective mutations in T_{NTD}, the T_{CTD} mutations do not cluster but are instead spread evenly across the entire domain. Most of the changes are dramatic alterations, representing charge changes (I88K, G148R, A158D, M190K, and I213K) or charge reversal (K120E). However, two conservative changes were also obtained: F78I and K137R. The conservative nature of the latter change suggests that position 137 dominates an intimate protein-protein interface. The most distal nonsense mutation obtained was at position 191 (Y191X), demonstrating that the extreme C-terminal 26 residues of T are required for lytic function. The I213K mutation is notable in that the mutation adds yet another positive charge to an already highly basic C-terminal polypeptide sequence (RILGRAK). This result contrasts with the case for both S105 and $S^{21}68$, where the extreme C-terminal domain is also rich in basic residues but is nonessential in both cases, although the timing of triggering is sensitive to the net charge (4).

Lysis-defective T proteins accumulate in the membrane. To determine whether the missense changes that confer an absolute lysis defect affect accumulation of the protein, whole-cell extracts taken at 15 min after induction were examined by immunoblotting with a T-specific antibody. Every allele tested exhibited normal T accumulation, with only a few showing slight reductions in T levels (Fig. 4A). Additionally, when cells from the induced cultures were collected, lysed, and fractionated to assay the soluble and membrane-bound levels of T, all of the lysis-defective mutants exhibited proper localization to the membrane (Fig. 4B). Studies with the other holin proteins have shown that similar variations of the level of holin accumulation affect lysis timing but not the capacity for hole formation (27). Thus, these defective *t* alleles are qualitatively dysfunctional, with the missense changes presumably affecting holin-holin interactions and blocking the hole formation pathway, as demonstrated for lysis-defective mutants of class I and II holins previously (13, 19).

Mutations conferring lysis defects are primarily in conserved residues. Residues important for the function and structure of a protein are usually conserved in their homologues. Thirty T homologues identified by BLAST analysis (28) were aligned to determine whether the lysis-defective missense mutations corresponded to conserved residues (Fig. 5). The result shows that while the T holins are well conserved in general, the residues at which mutations were isolated are conserved to an even higher degree. In particular, residues D19, F22, and F178 are more than 80% conserved, and residues I88, K137, and K148 are 100% conserved among the sequences analyzed.

Dominant and recessive character of lysis-defective mutants. The lysis-defective T holins were also tested for dominance-recessiveness by induction in the presence of prophage-borne wild-type T from a λ*t* hybrid prophage. In these experiments, dominant character was assigned if induction of a lysis-defective allele retarded lysis compared to that of the early nonsense mutant D19am (Fig. 6). By this criterion, only 3 alleles (I88K, A158D, and I213K) exhibited any dominant character. This result is significantly dif-

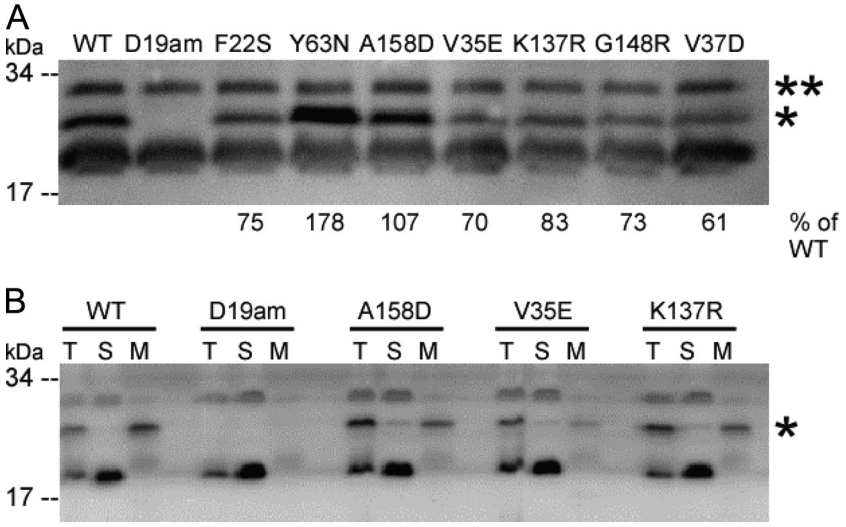

FIG 4 Lysis-defective mutants of T accumulate to wild-type T levels and are targeted to the membrane. (A) Western blot of whole-cell samples taken at 15 min after induction of the wild type, D19am (negative control), and various lysis-defective mutants of *t* as indicated. The percent protein accumulation of mutants compared to the wild type is indicated. (B) Membrane fractionation. The asterisk indicates a T-specific band. T, total protein; S, soluble fraction; M, membrane fraction.

ferent from the mutational analysis of S105 and $S^{21}68$, where numerous lysis-defective alleles were found to be at least partially dominant (2, 4). The simplest interpretation is that most *t* mutations that abolish lysis also disqualify the protein product from participating in the ultimate oligomerization.

Lysis-defective T mutants are defective in oligomerization. For S105, most lysis-defective alleles exhibited a defect in oligomerization (2). In order to characterize the oligomerization propensities of the wild-type and defective alleles of *t*, cross-linking experiments with dithiobis(succinimidyl propionate), glutaraldehyde, formaldehyde, and benzophenone-4-maleimide were carried out, similar to previous studies characterizing holin mutants (2, 11, 29). None of these methods allowed the detection of oligomeric species with wild-type T (not shown). To assess oligomerization with native protein, blue-native PAGE analysis of membrane extracts was performed. Membranes from cells induced for the wild-type or lysis-defective *t* alleles were extracted with 1% *n*-dodecyl-β-D-maltopyranoside (DDM) and characterized by blue-native PAGE. The wild-type sample had a discrete band at approximately 650 kDa, corresponding to ~27 T molecules (Fig. 7A). This observation was buttressed by gel filtration, where DDM micelles containing wild-type T eluted at ~900 kDa, calculated using a standard curve (Fig. 7B). This corresponds to ~34 T molecules (~25 kDa, each) based on a DDM aggregation number of 100 to 140 (micellar average molecular mass of 50 kDa) (11). By comparison, in blue-native PAGE, no discrete 650-kDa band was observed for six lysis-defective alleles, including 2 cytoplasmic domain mutants (F21 and L22) and 4 periplasmic domain mutants (Fig. 7A). For these mutant alleles, the T-specific species were spread across a wide mobility range (Fig. 7A). Moreover, when detergent extracts from two mutant alleles, one from each soluble domain (L21F and G148R), were analyzed by gel filtration, the 900-kDa micelle peak was completely missing (Fig. 7B). These results indicate that the lysis defects of these proteins reflect an inability to oligomerize, as previously shown for the products of S105 and $S^{21}68$ lysis-defective mutant alleles (2, 4, 30).

Previously, we showed that the purified periplasmic domain of T underwent aggregation and precipitation when eluted at high concentration from metal affinity columns (20). The protein could be rescued from precipitation by elution into solutions containing an excess of the periplasmic domain of the antiholin, RI, suggesting that precipitation reflected the antiholin-sensitive oligomerization function of the holin, rather than nonspecific aggregation. To determine whether the periplasmic domain mutants isolated in the context of the full-length protein affected this aggregation, the I88K mutation was introduced into a construct encoding T_{CTD}. When the mutant protein was overexpressed, bound to a metal affinity column, and eluted with imidazole, the

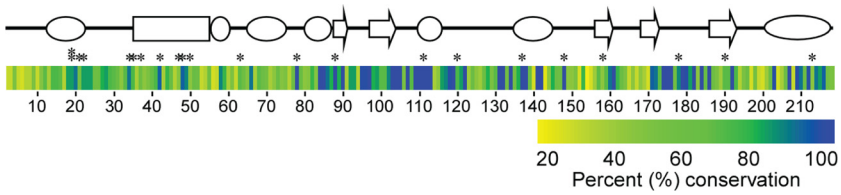

FIG 5 Lysis-defective mutations map primarily to the most conserved residues. The secondary structure elements of T are indicated with a heat map of the percent conservation of each residue based on an alignment of all T4-like phage holins. Asterisks indicate locations of nonfunctional mutants of the T4 holin. Conservation is based on alignments of the holin genes of T4 and the following T4-like phages: IME09, RB32, RB51, K3, Shfl2, RB14, Ar1, wV7, RB69, 133, Ac42, CC31, Acj61, Acj9, Bp7, IME08, JS10, VR7, SP18, JS98, 25, PhiAS4, 44RR2.8t, RB49, JSE, and RB16.

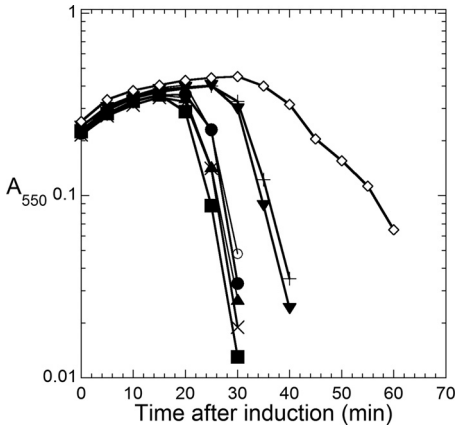

FIG 6 Certain mutants of T exhibit dominant character when coinduced with wild-type T. Wild-type *t* lysogens were induced for plasmid-borne *t* nonfunctional mutants. ■, wild type; ●, D19am (negative control); ▲, L21F; ▼, I88K; ×, F111S; +, A158D; ○, F178S; ◇, I213K. Mutants that exhibited delayed lysis compared to when the negative control was induced were characterized as those carrying dominant mutations.

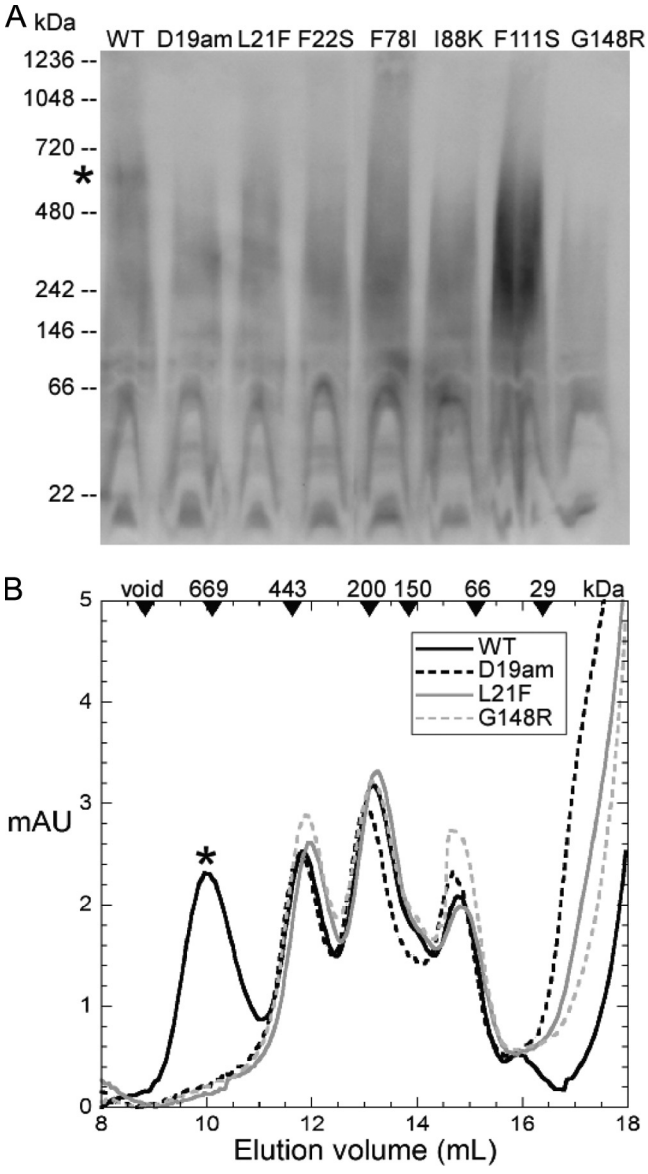

FIG 7 Nonlytic alleles of *t* are also defective in oligomerization. (A) Blue-native PAGE analysis of various nonfunctional alleles of T indicates that they are nonfunctional in oligomerization. The asterisk indicates migration of wild-type T. (B) Gel filtration of cell membrane extractions expressing WT or nonfunctional alleles of *t*. S-200 standards are indicated by arrowheads. The asterisk indicates a T-specific gel filtration peak.

protein remained soluble, even in the absence of the soluble RI domain (Fig. 8A). Gel filtration of the purified soluble protein confirmed that the T_{CTD} I88K protein had monomeric status (19 kDa) (Fig. 8B) Similar results were also obtained for another allele, I213K (not shown).

Lysis-defective alleles of T also defective in binding the anti-holin, RI. When lysis inhibition (LIN) is imposed, the lysis function of T is overridden by the binding of RI to the periplasmic domain of T (5, 20, 26). To assess whether any of the periplasmic domain T mutants were affected in RI binding, the 11 periplasmic domain mutants isolated in this study were transferred to a *phoA-t* chimera in which T_{CTD} is fused to the PhoA signal sequence. Expression of this chimera with the wild-type T_{CTD} during a T4 infection prevents LIN, due to the titration of RI by the soluble periplasmic domain of T (26). This phenotype was reproduced with 7 of the 11 mutants, indicating that these proteins are able to bind RI and prevent the onset of LIN (Fig. 2B). However, four alleles (I88K, F111S, K137R, and I213K) failed to block LIN. These results suggest that these positions are likely to be residues important for the T-RI interaction.

DISCUSSION

Here we have reported the selection and characterization of a collection of lysis-defective missense alleles of T4 *t*. Besides providing essential control materials for biochemical, biophysical, and cell biological analysis of T holin function, aspects of the distribution, location, and character of these lysis-defective mutations are informative, especially in terms of a comparison to the findings of previous detailed mutational studies on two prototype holins, the class I lambda S105 and the class II $S^{21}68$.

Distribution of lysis-defective mutations in *t*. By selecting for loss of lytic capacity, missense mutations were obtained in all three topological domains conferring functional defects without compromising the accumulation or subcellular localization of the mutant proteins. In contrast, all such mutations isolated in the S105 and $S^{21}68$ systems were located in the TMDs or connecting loops (2–4). In S105 and $S^{21}68$, the cytoplasmic and periplasmic oligopeptide sequences at the N and C termini have been shown to be regulatory domains, nonessential for hole formation (4, 31). Why is T different? First, T, like lambda S105, is a canonical, "large-hole-forming" holin. With canonical holins, it has been established that the product of triggering must be a very large lesion in the membrane, to allow fully folded, soluble endolysin to escape nonspecifically from the cytoplasm and attack the cell wall (32). More recently, the ultrastructural basis of this nonspecific release was established for two unrelated class I holins, lambda S105 and P2 Y, and also for T (9, 10). These studies showed the final holes to be of various sizes and on the scale of 100 to 1,000 nm in diameter. Assuming that the hole perimeter is lined with TMDs of the holins, thousands of holin molecules would be required to form the observed 1 to 3 holes per cell. In contrast, the pinholin $S^{21}68$ forms heptameric complexes with internal channels of ~2 nm,

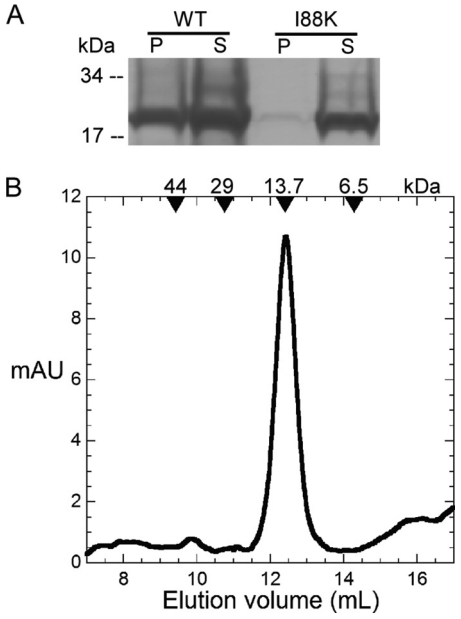

FIG 8 Periplasmic mutations causing loss of lytic function also confer an increase in solubility on T_{CTD}. (A) Purification of the WT T_{CTD} results in ~50% of protein remaining soluble, compared to ~100% for the I88K periplasmic domain mutant. (B) Gel filtration of T_{CTD} for I88K. The protein elutes in a single fraction consistent with monomeric status. S-75 standards are indicated by arrowheads. P, pellet; S, soluble.

which serve only to kill the cell and depolarize the membrane (11). What differentiates a canonical, large-hole-forming holin like S105 from a pinholin like $S^{21}68$? One difference is that S105 has three TMDs, all of which are required for hole formation (31). In contrast $S^{21}68$, at the time of hole formation, has only a single TMD, because, as part of the timing mechanism, the N-terminal TMD must be removed from the bilayer (19). Thus, it may be that a single TMD alone simply cannot form pores of micrometer scale as observed for the lambda holin, and, accordingly, that T, despite its single TMD, is able to achieve large-hole status by the participation of the periplasmic C-terminal domain. Indeed, the fact that the TMD lacks conservative mutations with lysis-defective phenotypes suggests that it may play a largely passive role in hole formation.

Homotypic and heterotypic interactions in T_{CTD}. T_{CTD}, spanning residues 56 to 216, is the location of 13 missense changes that abrogate T lethality without affecting accumulation or localization of the holin. Four of these alleles, in addition to causing loss of lytic function, also cause loss of the ability to bind the RI antiholin *in vivo* (Fig. 2B): I88K, F111S, K137R, and I213K. Moreover, to date two of these have been tested in the context of the purified, independent His-tagged T_{CTD}, and both have been shown to remain soluble after elution from an immobilized-metal affinity chromatograph (IMAC), in contrast to the wild-type T_{CTD}, which quantitatively oligomerizes to the point of insolubility upon elution (Fig. 8) (20). We suggest that these residues define an interface that is important for both homotypic T interactions leading to oligomerization and a heterotypic interaction with RI. This implies that RI acts by occluding one of the oligomerization interfaces used by T in the pathway to lethal hole formation, rather than by some allosteric effect on T conformation. Three of these changes are in highly conserved residues (Fig. 5). The allele K137R is of interest because of its extremely conservative nature. Among these positions, only I213 is not strongly conserved. However, even here a basic residue is not found in any T homologue.

Future exploitation of the lysis-defective allele collection. The collection of lysis-defective alleles of T can be exploited in several ways. First, they will provide controls for physiological and biochemical studies. This has been crucial for the studies of the S105 and S68 paradigms of the topological classes I and II. Membrane proteins are notorious for artifactual phenotypes due to excess synthesis or localization, so the stable missense mutants allow expression levels and protein concentrations to be calibrated for null holin function in physiological and biochemical experiments, respectively. Moreover, the absolute-defective alleles can be the starting reagents for intragenic suppression studies, by the simple expedient of selecting for restoration of lytic function. One would expect to obtain both true revertants and pseudorevertants, with the latter being the most informative at key sites of homo-oligomerization. Finally, the collections of defective alleles will also be invaluable in interpretation of crystal structures of the T protein. Experiments to this end are now in progress.

ACKNOWLEDGMENTS

This work was supported by Public Health Service grant GM-27099 (R.Y.) and by the Center for Phage Technology, an Initial University Multidisciplinary Research Initiative of Texas A&M University and Texas AgriLife.

We thank the Young lab members, past and present, for their helpful criticisms and suggestions.

REFERENCES

1. **Wang IN, Smith DL, Young R.** 2000. Holins: the protein clocks of bacteriophage infections. Annu. Rev. Microbiol. **54:**799–825. http://dx.doi.org/10.1146/annurev.micro.54.1.799.
2. **Gründling A, Bläsi U, Young R.** 2000. Genetic and biochemical analysis of dimer and oligomer interactions of the lambda S holin. J. Bacteriol. **182:**6082–6090. http://dx.doi.org/10.1128/JB.182.21.6082-6090.2000.
3. **Gründling A, Bläsi U, Young R.** 2000. Biochemical and genetic evidence for three transmembrane domains in the class I holin, lambda S. J. Biol. Chem. **275:**769–776. http://dx.doi.org/10.1074/jbc.275.2.769.
4. **Pang T, Park T, Young R.** 2010. Mutational analysis of the S21 pinholin. Mol. Microbiol. **76:**68–77. http://dx.doi.org/10.1111/j.1365-2958.2010.07080.x.
5. **Ramanculov E, Young R.** 2001. Genetic analysis of the T4 holin: timing and topology. Gene **265:**25–36. http://dx.doi.org/10.1016/S0378-1119(01)00365-1.
6. **Young R.** 2002. Bacteriophage holins: deadly diversity. J. Mol. Microbiol. Biotechnol. **4:**21–36.
7. **Park T, Struck DK, Deaton JF, Young R.** 2006. Topological dynamics of holins in programmed bacterial lysis. Proc. Natl. Acad. Sci. U. S. A. **103:**19713–19718. http://dx.doi.org/10.1073/pnas.0600943103.
8. **Gründling A, Manson MD, Young R.** 2001. Holins kill without warning. Proc. Natl. Acad. Sci. U. S. A. **98:**9348–9352. http://dx.doi.org/10.1073/pnas.151247598.
9. **Savva CG, Dewey JS, Moussa SH, To KH, Holzenburg A, Young R.** 2014. Stable micron-scale holes are a general feature of canonical holins. Mol. Microbiol. **91:**57–65. http://dx.doi.org/10.1111/mmi.12439.
10. **Dewey JS, Savva CG, White RL, Vitha S, Holzenburg A, Young R.** 2010. Micron-scale holes terminate the phage infection cycle. Proc. Natl. Acad. Sci. U. S. A. **107:**2219–2223. http://dx.doi.org/10.1073/pnas.0914030107.
11. **Pang T, Savva CG, Fleming KG, Struck DK, Young R.** 2009. Structure of the lethal phage pinhole. Proc. Natl. Acad. Sci. U. S. A. **106:**18966–18971. http://dx.doi.org/10.1073/pnas.0907941106.
12. **White R, Chiba S, Pang T, Dewey JS, Savva CG, Holzenburg A, Pogliano K, Young R.** 2011. Holin triggering in real time. Proc. Natl. Acad. Sci. U. S. A. **108:**798–803. http://dx.doi.org/10.1073/pnas.1011921108.
13. **To KH, Dewey J, Weaver J, Park T, Young R.** 2013. Functional analysis

of a class I holin, P2 Y. J. Bacteriol. **195:**1346–1355. http://dx.doi.org/10.1128/JB.01986-12.
14. **Hershey AD.** 1946. Mutation of bacteriophage with respect to type of plaque. Genetics **31:**620–640.
15. **Doermann AH.** 1948. Lysis and lysis inhibition with Escherichia coli bacteriophage. J. Bacteriol. **55:**257–276.
16. **Paddison P, Abedon ST, Dressman HK, Gailbreath K, Tracy J, Mosser E, Neitzel J, Guttman B, Kutter E.** 1998. The roles of the bacteriophage T4 r genes in lysis inhibition and fine-structure genetics: a new perspective. Genetics **148:**1539–1550.
17. **Dressman HK, Drake JW.** 1999. Lysis and lysis inhibition in bacteriophage T4: rV mutations reside in the holin t gene. J. Bacteriol. **181:**4391–4396.
18. **Ramanculov E, Young R.** 2001. Functional analysis of the phage T4 holin in a lambda context. Mol. Genet. Genomics **265:**345–353. http://dx.doi.org/10.1007/s004380000422.
19. **Pang T, Park T, Young R.** 2010. Mapping the pinhole formation pathway of S21. Mol. Microbiol. **78:**710–719. http://dx.doi.org/10.1111/j.1365-2958.2010.07362.x.
20. **Moussa SH, Kuznetsov V, Tran TA, Sacchettini JC, Young R.** 2012. Protein determinants of phage T4 lysis inhibition. Protein Sci. **21:**571–582. http://dx.doi.org/10.1002/pro.2042.
21. **Kuty GF, Xu M, Struck DK, Summer EJ, Young R.** 2010. Regulation of a phage endolysin by disulfide caging. J. Bacteriol. **192:**5682–5687. http://dx.doi.org/10.1128/JB.00674-10.
22. **Cole C, Barber JD, Barton GJ.** 2008. The Jpred 3 secondary structure prediction server. Nucleic Acids Res. **36:**W197–W201. http://dx.doi.org/10.1093/nar/gkn238.
23. **Krogh A, Larsson B, von Heijne G, Sonnhammer EL.** 2001. Predicting transmembrane protein topology with a hidden Markov model: application to complete genomes. J. Mol. Biol. **305:**567–580. http://dx.doi.org/10.1006/jmbi.2000.4315.
24. **Hofmann K, Stoffel W.** 1993. TMbase—a database of membrane spanning protein segments. Biol. Chem. Hoppe-Seyler **374:**166.
25. **Ramanculov E, Young R.** 2001. An ancient player unmasked: T4 rI encodes a t-specific antiholin. Mol. Microbiol. **41:**575–583. http://dx.doi.org/10.1046/j.1365-2958.2001.02491.x.
26. **Tran TA, Struck DK, Young R.** 2005. Periplasmic domains define holin-antiholin interactions in t4 lysis inhibition. J. Bacteriol. **187:**6631–6640. http://dx.doi.org/10.1128/JB.187.19.6631-6640.2005.
27. **Chang CY, Nam K, Young R.** 1995. S gene expression and the timing of lysis by bacteriophage lambda. J. Bacteriol. **177:**3283–3294.
28. **Altschul SF, Gish W, Miller W, Myers EW, Lipman DJ.** 1990. Basic local alignment search tool. J. Mol. Biol. **215:**403–410. http://dx.doi.org/10.1016/S0022-2836(05)80360-2.
29. **Zagotta MT, Wilson DB.** 1990. Oligomerization of the bacteriophage lambda S protein in the inner membrane of Escherichia coli. J. Bacteriol. **172:**912–921.
30. **Gründling A, Smith DL, Bläsi U, Young R.** 2000. Dimerization between the holin and holin inhibitor of phage lambda. J. Bacteriol. **182:**6075–6081. http://dx.doi.org/10.1128/JB.182.21.6075-6081.2000.
31. **White R, Tran TA, Dankenbring CA, Deaton J, Young R.** 2010. The N-terminal transmembrane domain of lambda S is required for holin but not antiholin function. J. Bacteriol. **192:**725–733. http://dx.doi.org/10.1128/JB.01263-09.
32. **Wang IN, Deaton J, Young R.** 2003. Sizing the holin lesion with an endolysin-beta-galactosidase fusion. J. Bacteriol. **185:**779–787. http://dx.doi.org/10.1128/JB.185.3.779-787.2003.